



## Phenolic phytochemical displaying SARS-CoV papain-like protease inhibition from the seeds of *Psoralea corylifolia*

Dae Wook Kim, Kyung Hye Seo, Marcus J. Curtis-Long, Kyeong Yeol Oh, Jong-Won Oh, Jung Keun Cho, Kon Ho Lee & Ki Hun Park

To cite this article: Dae Wook Kim, Kyung Hye Seo, Marcus J. Curtis-Long, Kyeong Yeol Oh, Jong-Won Oh, Jung Keun Cho, Kon Ho Lee & Ki Hun Park (2014) Phenolic phytochemical displaying SARS-CoV papain-like protease inhibition from the seeds of *Psoralea corylifolia*, Journal of Enzyme Inhibition and Medicinal Chemistry, 29:1, 59-63, DOI: [10.3109/14756366.2012.753591](https://doi.org/10.3109/14756366.2012.753591)

To link to this article: <https://doi.org/10.3109/14756366.2012.753591>



Published online: 16 Jan 2013.



Submit your article to this journal [↗](#)



Article views: 1230



View related articles [↗](#)



View Crossmark data [↗](#)



Citing articles: 14 View citing articles [↗](#)

RESEARCH ARTICLE

## Phenolic phytochemical displaying SARS-CoV papain-like protease inhibition from the seeds of *Psoralea corylifolia*

Dae Wook Kim<sup>1</sup>, Kyung Hye Seo<sup>2</sup>, Marcus J. Curtis-Long<sup>3</sup>, Kyeong Yeol Oh<sup>1</sup>, Jong-Won Oh<sup>4</sup>, Jung Keun Cho<sup>1</sup>, Kon Ho Lee<sup>2</sup>, and Ki Hun Park<sup>1</sup>

<sup>1</sup>Division of Applied Life Science (BK21 Program), IALS and <sup>2</sup>Department of Microbiology, School of Medicine, Gyeongsang National University, Jinju, Republic of Korea, <sup>3</sup>Graduate Program in Biochemistry and Biophysics, Brandeis University, Waltham, MA, USA, and <sup>4</sup>Department of Biotechnology, College of Life Science and Biotechnology, Yonsei University, Seoul, Republic of Korea

### Abstract

Severe acute respiratory syndrome coronavirus (SARS-CoV) papain-like protease (PLpro) is a key enzyme that plays an important role in SARS virus replication. The ethanol extract of the seeds of *Psoralea corylifolia* showed high activity against the SARS-CoV PLpro with an IC<sub>50</sub> of value of 15 µg/ml. Due to its potency, subsequent bioactivity-guided fractionation of the ethanol extract led to six aromatic compounds (1–6), which were identified as bavachinin (1), neobavaisoflavone (2), isobavachalcone (3), 4'-O-methylbavachalcone (4), psoralidin (5) and corylifol A (6). All isolated flavonoids (1–6) inhibited PLpro in a dose-dependent manner with IC<sub>50</sub> ranging between 4.2 and 38.4 µM. Lineweaver–Burk and Dixon plots and their secondary replots indicated that inhibitors (1–6) were mixed inhibitors of PLpro. The analysis of K<sub>i</sub> and K<sub>iS</sub> values proved that the two most promising compounds (3 and 5) had reversible mixed type I mechanisms.

### Keywords

Mixed type I inhibition, papain-like protease inhibitor, *Psoralea corylifolia*, severe acute respiratory syndrome coronavirus papain-like protease

### History

Received 3 November 2012  
Revised 25 November 2012  
Accepted 25 November 2012  
Published online 16 January 2013

Severe acute respiratory syndrome coronavirus (SARS-CoV) is a zoonotic RNA virus that is highly contagious and causes fatal respiratory illness. SARS-CoV has been controlled by inhibiting a number of significant targets involved in viral replication. SARS-CoV has been controlled by inhibiting a number of significant targets involved in viral replication. An early and essential process of SARS-CoV replication is the cleavage of a multidomain viral polyprotein into 16 mature components required for viral RNA synthesis<sup>1</sup>. It is well known that two cysteine proteases, a papain-like protease (PLpro) and a 3C-like protease are the key players in this maturation process<sup>2</sup>. These two proteases catalyze their own release and liberate other nonstructural proteins from the polyprotein. Recent structural and functional studies directed at PLpro have suggested potential roles for this protease beyond viral peptide cleavage, including deubiquitination, deISGylation and involvement in virus evasion of the innate immune response<sup>3–5</sup>. The numerous functions of PLpro in viral replication and pathogenesis suggest that PLpro may serve as an attractive target for antiviral drugs. Many rationally designed compounds have been developed as inhibitors of SARS-CoV PLpro. However, natural compounds exhibiting SARS-CoV PLpro inhibition activity are yet to be reported.

During an intensive research program into biologically active metabolites from *Psoralea corylifolia*, we found that the ethanol

extract showed significant inhibition against SARS-CoV PLpro. *Psoralea corylifolia* belongs to the Leguminosae family, the seeds of which are a permitted food additive in many countries, especially South Korea. The major bioactive components of the seeds of *P. corylifolia* are flavonoids and chalcones, including bavachinin, psoralidin, and isobavachalcone<sup>6</sup>. Moreover, the constituents of *P. corylifolia* have been found to exhibit antioxidant, antibacterial, anti-inflammatory and antidepressant activities<sup>7–9</sup>. *Psoralea corylifolia* has also been reported to have inhibitory activities of baculovirus-expressed BACE-1, DNA polymerase and topoisomerase II<sup>10,11</sup>. We also reported glycosidase inhibitory phenolic compounds from this species<sup>12</sup>.

In this study, we isolated six aromatic compounds targeting SARS-CoV PLpro from the seeds of *P. corylifolia*. The isolated compounds were evaluated separately for their inhibitory activities against PLpro. Their inhibition mechanisms were ascertained using Lineweaver–Burk and Dixon plots. The literature revealed that no such work has been reported on the seeds of *P. corylifolia*.

### Materials and methods

#### Plant material, extraction and isolation

The dried seeds (1 kg) of *P. corylifolia* were purchased from the local market and extracted with ethanol (2 l) three times at room temperature. The ethanol soluble portion was concentrated to give the crude extract (87 g), which was partitioned between H<sub>2</sub>O and *n*-hexane. The aqueous layer was further partitioned with EtOAc to give the EtOAc extract (59 g), which was subjected to MPLC

Address for correspondence: Ki Hun Park, Division of Applied Life Science (BK21 Program), IALS, Gyeongsang National University, Jinju 660701, Republic of Korea. Tel: +82 55 7721965. Fax: +82 55 7721969. E-mail: khpark@gnu.ac.kr

on a silica gel column with a gradient solvent system of *n*-hexane–CHCl<sub>3</sub>–MeOH to provide six fractions (A–F). Potent inhibition targeting to PLpro was found on fraction C that was further chromatographed on a Sephadex LH-20 (Piscataway, NJ) column with MeOH as the eluent to give five main fractions (Fr1–Fr5). The Fr2 was purified by silica gel column (230–400 mesh) chromatography with a gradient solvent system of *n*-hexane–acetone (100:0–10:1) to afford psoralidin (18 mg, **5**) and corylifol A (15 mg, **6**). The Fr3 was chromatographed with a gradient solvent system of *n*-hexane–EtOAc (50:1–5:1) to yield four sub-fractions (Fr3-1–Fr3-4). The Fr3-2 was separated to more six fractions (Fr3-2-1–Fr3-2-6) by ODS column chromatography with 80% MeOH as the eluent. The Fr3-2-1 was further purified on a silica gel column with CHCl<sub>3</sub>–EtOAc (100:1–30:1) as the eluent to afford isobavachalcone (42 mg, **3**) and 4'-*O*-methylbavachalcone (31 mg, **4**). The Fr3-2-3 was purified on a Sephadex LH-20 column with MeOH as eluent to give isobavachromene neobavaisoflavone (18 mg, **2**). Another main fraction (Fr6) was subject to silica gel column chromatography eluting with CHCl<sub>3</sub>–acetone (50:1–10:1) to yield seven sub-fractions (Fr6-1–Fr6-7). The Fr6-1 was chromatographed on a Sephadex column with CH<sub>2</sub>Cl<sub>2</sub>–MeOH (1:4) as the eluent and more five fractions (Fr6-1-1–Fr6-1-5) were obtained. The Fr6-1-4 was separated by ODS with 70% MeOH in H<sub>2</sub>O as the solvent system to give bavachinin (13.2 mg, **1**). The chemical structures of these compounds were determined by comparison of their spectroscopic data with those previously reported<sup>13</sup>.

#### Expression and purification of SARS-CoV PLpro from *Escherichia coli*

The PLpro gene (945 bp) was PCR amplified from the plasmid pSARS-REP and plasmid pProEx HT expression vector (Invitrogen, Carlsbad, CA) and transformed into DH5 $\alpha$  competent cells. The expression plasmid was constructed such that PLpro carried an *N*-terminal His<sub>6</sub>-tag followed by a tobacco etch virus protease (TEV) site. Correct clones containing the PLpro gene in a pProEX HT vector were identified and verified by PCR and restriction digestion with *Bam*HI and *Xho*I. The plasmid pProEX HT harboring the PLpro gene was transformed into BL21(DE3) *E. coli* (Novagen, Madison, WI). A 10 ml aliquot of an overnight culture was seeded into 1000 ml of fresh Luria–Bertani medium containing 50 mg/ml ampicillin and cells were grown to an OD<sub>600 nm</sub> of 0.6 at 37 °C. The cells were cooled on ice for 30 min and protein expression was induced for 5 h with 0.4 mM isopropyl  $\beta$ -D-1-thiogalactopyranoside at 30 °C. The cells were harvested by centrifugation at 6000 rpm for 6 min at 4 °C. The harvested cells

were washed twice in phosphate-buffered saline. The cell pellet was used directly for purification or stored at –80 °C until use.

The cell pellet was suspended in binding buffer (50 mM NaH<sub>2</sub>PO<sub>4</sub> pH 8.0, 500 mM NaCl, 5 mM imidazole and 5 mM  $\beta$ -mercaptoethanol) and cells were disrupted by sonication. After centrifugation at 15000 rpm for 1 h, the clear supernatant was collected, filtered (Advantec, Saijyo, Ehime, Japan) and applied onto a column of Nickel Sepharose 6 Fast Flow (GE Healthcare, Stockholm, Sweden) beads pre-equilibrated with the binding buffer. The column was washed first with 20 column volumes of binding buffer and then with 2 column volumes of washing buffer (50 mM Tris–HCl pH 8.0, 500 mM NaCl and 30 mM imidazole). Recombinant PLpro was eluted with elution buffer (50 mM Tris–HCl pH 8.0, 100 mM NaCl and 300 mM imidazole). Eluted PLpro was further purified by ion-exchange chromatography using a salt gradient with a SOURCE 15Q column (GE Healthcare, Piscataway, NJ) in 50 mM Tris–HCl pH 8.5 and 2 mM DTT. PLpro was finally purified by size exclusion chromatography on a Superdex 200 column (GE Healthcare, Piscataway, NJ) in 20 mM Tris–HCl pH 8.0, 150 mM NaCl and 2 mM DTT. The fractions containing PLpro were pooled, exchanged into 20 mM Tris–HCl pH 8.0 and 10 mM DTT and concentrated to a final concentration of 10 mg/mL by ultrafiltration (Microcon YM-30, Millipore Corporation, Bedford, MA). The protein purity was examined by SDS-PAGE and native-PAGE. The protein concentration was determined by Bradford assay<sup>14</sup> using bovine serum albumin as the standard. The *N*-terminal his-tag was removed by TEV digestion prior to activity assays.

#### SARS-CoV PLpro inhibition assay

IC<sub>50</sub> values for all inhibitors were determined using a 96-well plate-based assay similar to our previously reported procedures<sup>15,16</sup>. The substrate used in the assay was the fluorogenic peptide Z-Arg-Leu-Arg-Gly-Gly-7-amido-4-methylcoumarin (Z-RLRGG-AMC), which was purchased from ENZO Life Sciences (Farmingdale, NY). The substrate contains the five C-terminal residues of human ubiquitin with a C-terminal AMC group. Hydrolysis of the AMC–peptide bond dramatically increases the fluorescence of the AMC moiety, allowing conversion to be accurately determined. Reactions were performed in a total volume of 200  $\mu$ L, which contained the following components: 20 mM Tris-buffer, pH 8.0, 10 mM DTT, 30  $\mu$ M Z-RLRGG-AMC, 2% DMSO and varying concentrations of inhibitor (0–200  $\mu$ M). Assays were initiated with the addition of PLpro to produce a final enzyme concentration of 60 nM. Reaction progress was monitored continuously on a SpectraMax

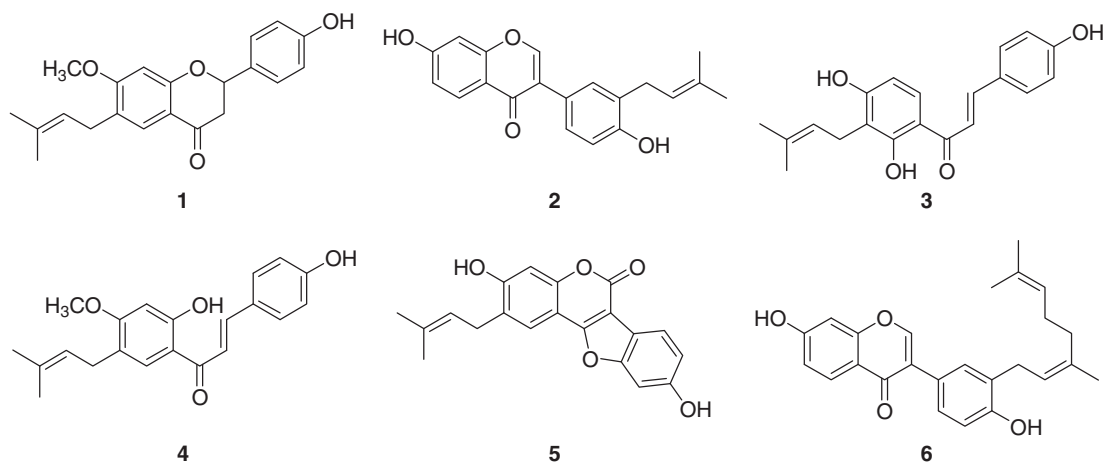


Figure 1. Chemical structures of isolated PLpro inhibitors **1–6**.

M3Multi-Mode Microplate Reader (Sunnyvale, CA) ( $\gamma_{\text{excitation}} = 360 \text{ nm}$ ;  $\gamma_{\text{emission}} = 460 \text{ nm}$  and gain = 40) and the reaction rate was calculated by the equation  $vi = vo/(1 + [I]/IC_{50})$  using the enzyme kinetics module of Sigma Plot (v. 9.01 Systat Software, Inc., Chicago, IL) where  $vi$  is the reaction rate in the presence of inhibitor,  $vo$  the reaction rate in the absence of inhibitor and  $[I]$  the inhibitor concentration.

### Enzyme kinetic assay and progress linear determination

The inhibition kinetics of the enzyme by the isolated compounds were analyzed by Lineweaver–Burk plots and compared to data obtained in the absence of inhibitor. To determine the kinetic parameters associated with inhibition mechanism of PLpro, steady-state rates were obtained at several inhibitor concentrations and varying substrate concentrations. The two inhibition constants for inhibitor binding with either free or enzyme–substrate complex,  $K_I$  or  $K_{IS}$ , were obtained from secondary plots of the slopes of the straight lines or vertical intercept ( $1/V_{\text{max}}^{\text{app}}$ ), respectively, versus the concentration of inhibitors.  $K_I$  and  $K_{IS}$  are represented by Equations (1)–(3), respectively<sup>17,18</sup>:

$$1/V = K_m/V_{\text{max}}(1 + [I]/K_I)1/S + 1/V_{\text{max}} \quad (1)$$

$$\text{Slope} = K_m/K_I V_{\text{max}}[I] + K_m/V_{\text{max}} \quad (2)$$

$$\text{Intercept} = 1/V_{\text{IS}} V_{\text{max}}[I] + 1/V_{\text{max}} \quad (3)$$

### Statistical analysis

All measurements were made in triplicate. The results were subject to variance analysis using Sigma plot. Differences were considered significant at  $p < 0.05$ .

### Results and discussion

In preliminary screening, we observed that the ethanol extract of *P. corylifolia* seeds showed significant inhibition ( $IC_{50} = 15 \mu\text{g/ml}$ ) of SARS-CoV PLpro. Activity-guided fractionation of the ethanol extract gave six flavonoids (1–6), which were purified over silica gel, Sephadex LH-20, and octadecyl-functionalized silica gel as delineated above. Isolated compounds (1–6) were identified as the known species bavachinin (1), neobavaisoflavone (2), isobavachalcone (3), 4'-O-methylbavachalcone (4), psoralidin (5) and corylifol A (6) through analysis of spectroscopic data and comparison with previous studies (Figure 1). Especially, molecular formulas, degrees of unsaturation and number of rings for each compounds were confirmed by  $^{13}\text{C}$ -NMR and HREIMS:  $m/z$  338.1520  $[M]^+$  for 1;  $m/z$  322.1204  $[M]^+$  for 2;  $m/z$  324.1635  $[M]^+$  for 3;  $m/z$  338.1519  $[M]^+$  for 4;  $m/z$  336.0995  $[M]^+$  for 5 and  $m/z$  390.1836  $[M]^+$  for 6.

The SARS-CoV PLpro (residues 154–1855) was expressed in *E. coli* and purified by successive nickel affinity, ion-exchange and gel filtration chromatography. The last step was used to separate the desired monomer from larger oligomers. The mass of the isolated PLpro was confirmed by MALDI-TOF. The His<sub>6</sub>-tag used for purification was removed by TEV cleavage. Activity of the purified PLpro was demonstrated by its ability to cleave a fluorogenic peptide substrate (supplementary materials). The apparent Michaelis–Menten constant ( $K_m = 30 \pm 0.9 \mu\text{M}$ ) was determined by plotting the initial rates corrected for the enzyme concentration (60 nM) versus substrate concentration (5–320  $\mu\text{M}$ ) and fitting the data to the Michaelis–Menten model (supplementary materials).

All isolated flavonoids (1–6) inhibited PLpro in a dose-dependent manner with  $IC_{50}$ s ranging between 4.2 and 38.4  $\mu\text{M}$  (Table 1 and Figure 2A). However, two representative secondary metabolites of *P. corylifolia*, psoralen and isopsoralen (both

Table 1. Inhibitory effects of compounds 1–6 on PLpro activity.

Compound	$IC_{50}^*$ value ( $\mu\text{M}$ )	Inhibition mode ( $K_I$ , $K_{IS} \mu\text{M}$ ) <sup>†</sup>
1	$38.4 \pm 2.4$	Mixed ( $18.4 \pm 1.7$ )
2	$18.3 \pm 1.1$	Mixed ( $9.4 \pm 0.8$ )
3	$7.3 \pm 0.8$	Mixed ( $4.9 \pm 0.9$ , 9.1)
4	$10.1 \pm 1.2$	Mixed ( $4.6 \pm 1.0$ )
5	$4.2 \pm 1.0$	Mixed ( $1.7 \pm 0.4$ , 4.2)
6	$32.3 \pm 3.2$	Mixed ( $11.4 \pm 2.5$ )
Psoralen	>150	NT <sup>‡</sup>
Isopsoralen	>150	NT

\*All compounds were examined in a set of experiments repeated three times;  $IC_{50}$  values of compounds represent the concentration that caused 50% enzyme activity loss, <sup>†</sup>values of inhibition constant and <sup>‡</sup>not tested.

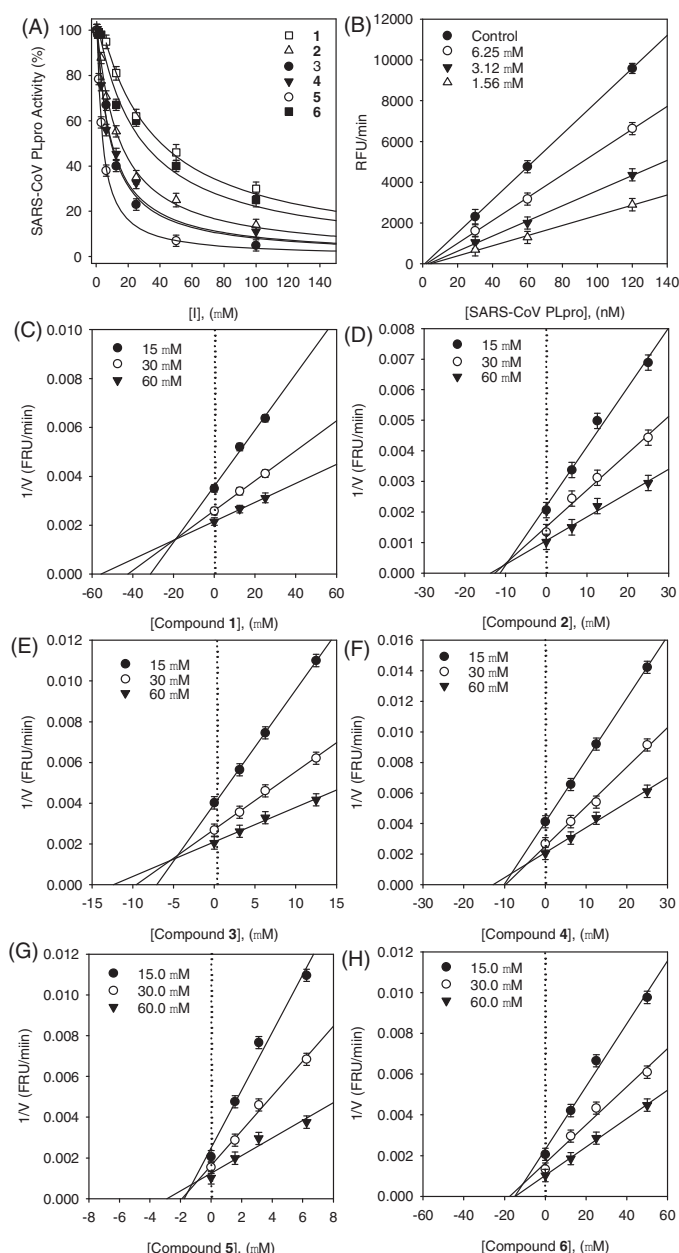


Figure 2. (A) Effects of isolated compounds 1–6 on SARS-CoV PLpro for the hydrolysis of Z-RLRGG-AMC, (B) the catalytic activity of SARS-CoV PLpro as a function of enzyme concentration at different concentrations of compound 5 and (C–H) Dixon plots for the inhibition of compounds (1–6), respectively, on the hydrolysis activity of PLpro in the presence of different concentrations of substrate.



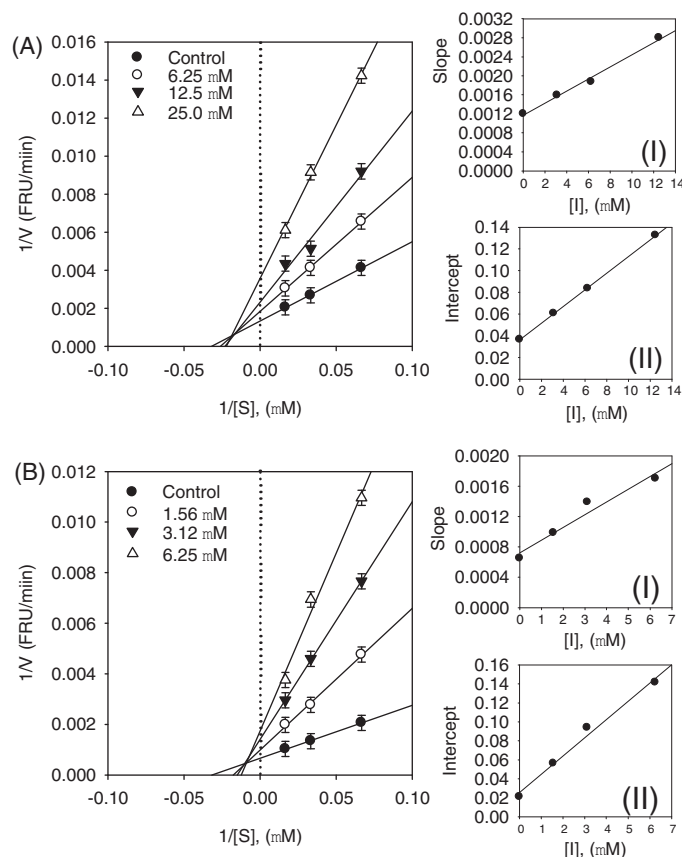


Figure 3. (A–B) Kinetic assays of SARS-CoV PLpro inhibition by isobavachalcone (**3**) and psoralidin (**5**). Lineweaver–Burk plots were constructed for the inhibition of SARS-CoV PLpro by compounds (**3** and **5**). The plot is expressed as  $1/\text{velocity}$  versus  $1/\text{PLpro}$  ( $\text{nM}^{-1}$ ) with or without inhibitor. Insets (I) and (II) represent the secondary plot of the slope and the intercept of the straight lines versus concentration of compounds (**3** and **5**), respectively.

unfunctionalized furocoumarins) were inactive against PLpro up to  $150\text{ }\mu\text{M}$ . Coumestrol (**5**) was found to be the most potent inhibitor with an  $\text{IC}_{50}$  of  $4.2\text{ }\mu\text{M}$ . Chalcones (**3** and **4**) exhibited a significant degree of inhibition ( $\text{IC}_{50} = 7.3\text{--}10.1\text{ }\mu\text{M}$ ) in comparison to flavanones (**1**) and isoflavones (**2** and **6**). The  $K_I$  values of all compounds were determined to fall within the range  $1.7\text{--}18.4\text{ }\mu\text{M}$ , from the common x-axis intercept of lines on the corresponding Dixon plots (Figure 2C–H). Kinetic assays were repeated in the presence of different concentrations ( $1\text{--}150\text{ }\mu\text{M}$ ) of compounds (**1–6**) to characterize inhibition of Z-RLRGG-AMC hydrolysis. The inhibition of PLpro by compound **5** (the most effective species) is shown in Figure 2(B), representatively. Plots of the initial velocity versus enzyme concentration in the presence of different concentrations of compound **5** gave a family of straight lines, all of which passed through the origin. Increasing the inhibitor concentration resulted in lowering of the slope of the line, indicating that compound **5** is a reversible inhibitor (Figure 2B). Other tested inhibitors (**1–4** and **6**) showed a similar profile to **5**.

The enzyme inhibition properties of these derivatives were modeled using double-reciprocal plots (Lineweaver–Burk and Dixon analyses). As shown in Figure 3(A) and (B), the inhibition kinetics analyzed by Lineweaver–Burk plots show that compounds **3** and **5** are mixed-type inhibitors because increasing inhibitor concentration resulted in a family of lines which intersected at a nonzero point on both x- and y-axes. The equilibrium constant for inhibitor binding,  $K_I$  was obtained from

the value at the intersection of three lines from Dixon plots (Figure 2C–H). The  $K_I$  values of inhibitors are presented in Table 1.

Since the inhibition was mixed, this means that the inhibitor has different affinities for the substrate bound and free enzyme. We thus sought to parse out the respective inhibition constants for the two states, which are referred to as type I, where inhibitor preferably binds to the free enzyme, or type II, where the inhibitor preferentially binds to the enzyme substrate complex. This analysis is carried out by varying both inhibitor and substrate concentration, as shown by Equations (1)–(3). The equilibrium constants for the two different binding events, inhibitor binding to free enzyme ( $K_I$ ) and enzyme–substrate complex ( $K_{IS}$ ) were obtained from secondary plots of  $K_m/V_{\text{max}}$  and  $1/V_{\text{max}}$  versus concentration of compounds **3** and **5**, respectively. We thus established the following constants: compound **3**,  $K_I = 4.9\text{ }\mu\text{M}$ , and  $K_{IS} = 9.5\text{ }\mu\text{M}$ ; compound **5**,  $K_I = 1.7\text{ }\mu\text{M}$  and  $K_{IS} = 4.2\text{ }\mu\text{M}$  (Figure 3 insets). These data show that the affinity of the inhibitor for free enzyme is marginally stronger than the affinity of inhibitor for the enzyme–substrate complex. Thus, compounds **3** and **5** are mixed type I inhibitors.

This study demonstrates that the ethanol extract of *P. corylifolia* seeds shows potent inhibitory activity toward SARS-CoV PLpro. Purification of this fraction gave six phenolic phytochemicals that displayed good PLpro inhibitory activities. These data validate *P. corylifolia* as rich source of potent PLpro inhibitors. Two compounds, isobavachalcone (**3**), and psoralidin (**5**) were the principal contributors to the PLpro inhibition. The analysis of  $K_I$  and  $K_{IS}$  values proved that the two most promising compounds (**3** and **5**) had a reversible mixed type I behavior.

## Declaration of interest

The authors have declared that there is no conflict of interest.

This study was supported by National Research Foundation Grant funded by Korea government (MEST; no. 2012-0001112) and Technology Development Program for Agriculture and Forestry (308025-05-4-HD110), Ministry for Food, Agriculture, Forestry and Fisheries, Republic of Korea. All students were supported by BK21 program.

## References

- Ziebuhr J. The coronavirus replicase. *Curr Top Microbiol Immunol* 2005;287:57–94.
- Ratia K, Pegan S, Takayama J, et al. A noncovalent class of papain-like protease/deubiquitinase inhibitors blocks SARS virus replication. *Proc Natl Acad Sci USA* 2008;105:16119–24.
- Devaraj SG, Wang N, Chen Z, et al. Regulation of IRF-3-dependent innate immunity by the papain-like protease domain of the severe acute respiratory syndrome coronavirus. *J Biol Chem* 2007;282:32208–21.
- Ratia K, Saikatendu KS, Santarsiero BD, et al. Severe acute respiratory syndrome coronavirus papain-like protease: structure of a viral deubiquitinating enzyme. *Proc Natl Acad Sci USA* 2006;103:5717–22.
- Barretto N, Jukneliene D, Ratia K, et al. The papain-like protease of severe acute respiratory syndrome coronavirus has deubiquitinating activity. *J Virol* 2005;79:15189–98.
- Xiao G, Li G, Chen L, et al. Isolation of antioxidants from *Psoralea corylifolia* fruits using high-speed counter-current chromatography guided by thin layer chromatography-antioxidant autographic assay. *J Chromatogr A* 2010;1217:5470–6.
- Guo JM, Weng XC, Wu H, et al. Antioxidants from a Chinese medicinal herb – *Psoralea corylifolia* L. *Food Chem* 2005;91:287–92.
- Khatune NA, Islam ME, Haque ME, et al. Antibacterial compounds from the seeds of *Psoralea corylifolia*. *Fitoterapia* 2004;75:228–30.

9. Xu Q, Pan Y, Yi LT, et al. Antidepressant-like effects of psoralen isolated from the seeds of *Psoralea corylifolia* in the mouse forced swimming test. *Biol Pharm Bull* 2008;31:1109–14.
10. Choi YH, Yon GH, Hong KS, et al. In vitro BACE-1 inhibitory phenolic components from the seeds of *Psoralea corylifolia*. *Planta Med* 2008;74:1405–8.
11. Sun NJ, Woo SH, Cassady JM, Snapka RM. DNA polymerase and topoisomerase II inhibitors from *Psoralea corylifolia*. *J Nat Prod* 1998;61:362–6.
12. Oh KY, Lee JH, Curtis-Long MJ, et al. Glycosidase inhibitory phenolic compounds from the seed of *Psoralea corylifolia*. *Food Chem* 2010;121:940–5.
13. Hisashi M, Sachie K, Sachiko S, et al. Inhibition from the seeds of *Psoralea corylifolia* on production of nitric oxide in lipopolysaccharide-activated macrophages. *Biol Pharm Bull* 2009;32:147–9.
14. Bradford MM. A rapid and sensitive method for the quantization of microgram quantities of protein utilizing the principle of protein-dye binding. *Anal Biochem* 1976;72:248–54.
15. Sulea T, Lindner HA, Purisima EO, Ménard, R. Deubiquitination, a new function of the severe acute respiratory syndrome coronavirus papain-like protease? *J Virol* 2005;79:4550–1.
16. Lindner HA, Fotouhi-Ardakani N, Lytvyn V, et al. The papain-like protease from the severe acute respiratory syndrome coronavirus is a deubiquitinating enzyme. *J Virol* 2005;79:15199–208.
17. Zhang JP, Chen QX, Song KK, Xie JJ. Inhibitory effects of salicylic acid family compounds on the diphenolase activity of mushroom tyrosinase. *Food Chem* 2006;95:579–84.
18. Chiari ME, Vera DMA, Palacios SM, Carpinella MC. Tyrosinase inhibitory activity of a 6-isoprenoid-substituted flavanone isolated from *Dalea elegans*. *Bioorg Med Chem* 2011;19:3474–82.